Metal-Dimer Atomic Reconstruction Leading to Deep Donor States of the Anion Vacancy in II-VI and Chalcopyrite Semiconductors

Stephan Lany and Alex Zunger

National Renewable Energy Laboratory, Golden, Colorado 80401, USA

First-principles total-energy calculations reveal a novel local atomic reconstruction mode around anion vacancies in II-VI and chalcopyrite compounds resulting from the formation of metal dimers. As a consequence, the neutral Se vacancy has an unexpected low symmetry in ZnSe and becomes a deep donor in both ZnSe and CuGaSe$_2$, contrary to the common belief regarding chalcopyrites. The calculated optical transition energies explain the hitherto puzzling absorption bands observed in the classic experiments of the color center in ZnS.

      PACS numbers: 71.15.Mb, 71.20.Nr, 71.55.Gs

Vacancies are the most fundamental point defects in solids, controlling mechanical properties in metals [1] and electrical properties in semiconductors [2]. While in homopolar IV-IV semiconductors vacancies produce deep (recombination) centers [2,3], in III-V and II-VI compound semiconductors vacancies can produce shallow states that are capable of releasing free carriers [2,4]. *Anion-site* vacancies are important technologically for their concentration is readily controlled during growth via the anion-source vapor pressure, affording direct control of the free electron density when the anion vacancy produces shallow donor levels. Whereas the Se vacancy V_{Se} in ZnSe was predicted to create a deep donor level [5,6], other anion vacancies are often thought to be shallow [4]. Indeed it has long been believed that the oxygen vacancy in ZnO yields a shallow donor state, which renders this material metalliclike *n*-type, serving as a "natural dopant", which produces a "transparent conductor" [4,7]. Similarly, in the ternary analog of II-VI semiconductors—the chalcopyrite family (e.g., CuInSe$_2$ and CuGaSe$_2$)—, shallow donor states have been attributed to the anion vacancy on the basis of electrical and optical measurements [8,9], as well as theoretical investigations [10]. The expectation that the anion vacancy produces a shallow level has guided growth and design of chalcopyrite solar cells [11,12]. Furthermore, since the neutral anion vacancies in II-VI materials create a closed-shell a_1^2 (He-like) electronic configuration, it was expected theoretically [13] that the atomic configuration around the vacancy would be symmetric (i.e., no Jahn-Teller distortion).

Using first-principles supercell calculations on the Se vacancy in ZnSe, we find a highly nonsymmetric atomic configuration, with lower point-group symmetry (C_{2v}) and 0.32 eV lower total energy than the symmetry-conserving (T_d) configuration underlying the tetrahedral zinc blende lattice. This geometry was discovered during energy-minimizing atomic relaxation simulations by starting from highly nonsymmetric atomic configurations, rather than from the traditional, near-T_d starting

point. This symmetry lowering is driven by the energetically stable formation of Zn-Zn dimer bonds around the anion vacancy. For V_{Se} in CuGaSe$_2$, we find the formation of an even stronger Ga-Ga dimer bond next to the anion vacancy. As a result of these strong atomic reconstructions, we find that the anion vacancies become *deep donors* with electrical levels located in the lower part of the band gap, incapable of producing free electrons. This is an important result, for it suggests that the prevailing view that anion vacancy control would make chalcopyrites *n*-type [8,10–12], has to be discarded. Furthermore, our discovery of metastable configurations associated with large lattice relaxations can account for the previously puzzling phenomenon of *p*-type "persistent photoconductivity" observed in chalcopyrite Cu(In, Ga)Se$_2$ photovoltaic devices [12]. The formation of deep anion vacancy orbitals in II-VIs explains the absorption bands which result in excitation and quenching of the electron paramagnetic resonance (EPR) in the classic experiments of the color center in ZnS [14] and in newer experiments in ZnSe [15], without the need to invoke other defects, as originally proposed [14,15].

Method— We use 64 atom supercell calculations in order to determine for the anion vacancy the atomic structure, the electronic structure (single-particle defect levels), defect formation energy ΔH_f (cp. e.g., Ref. [10]), and optical transition energies. The total-energy E and atomic forces were calculated in the pseudopotential-momentum space formalism [16] within the local density approximation (LDA) of density functional theory. We use the Ceperley-Alder LDA exchange correlation potential as parameterized by Perdew and Zunger [17] and projector augmented wave potentials as implemented in the VASP code [18]. The energy cutoff in the plane-wave expansion was 280 eV, and Brillouin zone integrations were performed on a $3 \times 3 \times 3$ mesh using the improved tetrahedron method. In case of the charged vacancies, the spurious interaction of periodic image charges is corrected to $O(L^{-5})$ [19], where L is the linear supercell dimension. We use the experimental lattice constants of

ZnSe and CuGaSe$_2$ [20]. The LDA band gap error is corrected first by acknowledging that the cation d states in II-VIs and chalcopyrites are too shallow on account of their strong, spurious self-interaction [17(b)]. Thus, we use the LDA+U method [21] to lower the Zn $3d$ and Cu $3d$ bands so as to yield agreement of the density of states with Zn and Cu photoemission data in ZnSe and CuGaSe$_2$ [22], respectively. This d-band lowering weakens the p-d-repulsion with the anion-p orbitals [23], thus lowering the energy of the valence band maximum (VBM) E_v and increasing the band gap of ZnSe by 0.28 eV and that of CuGaSe$_2$ by 0.37 eV. The remaining discrepancy between the LDA+U band gaps (1.35 and 0.4 eV) and the measured ones (2.8 and 1.7 eV) was accommodated by shifting the conduction band (CB) minimum upwards. The shift of the conduction band states was not applied to the donor level of the vacancy, because it is not expected to follow the CB due to the localized, bondinglike nature of the occupied vacancy orbital [24].

Asymmetric atomic configuration and formation of metal dimers— Removal of a neutral column VI element from the II-VI lattice creates a doubly occupied, closed-shell a_1^2 level. It was thus not expected that any Jahn-Teller type symmetry-lowering (akin, e.g., to the open-shell $a_1^2 t_2^1$ configuration of V_{anion} in III-Vs [2]) would take place [6,13]. Accordingly, the energy gain of V_{Se}^0 in ZnSe associated with symmetry lowering from T_d to trigonal (C_{3v}) calculated by Pöykkö *et al.* [6], was left unexplained. We investigate here the different possible relaxation modes of V_{Se}^0 in ZnSe and CuGaSe$_2$ (lower part of Fig. 1). For ZnSe, we find, in agreement with Pöykkö *et al.* [6], that the C_{3v} relaxation mode of V_{Se}^0 in ZnSe (not shown in Fig. 1) is more stable than the tetrahedral mode by 0.16 eV. However, an orthorhombic (C_{2v}) relaxation mode (Fig. 1), is found to be even more stable, being 0.32 eV lower than the symmetric T_d configuration (Table I) [20]. Interestingly, the T_d mode is found to be an unstable (albeit force free) configuration in that it decays without activation into the C_{2v} state after application of a normal mode distortion consisting of an orthorhombic expansion of two of the four Zn-Zn distances next to the vacancy. Analysis of the wave functions shows that the a_1 state is constructed from a bondinglike combination of two, three, or four Zn dangling bond orbitals in the C_{2v}, C_{3v}, and T_d symmetry, respectively. In CuGaSe$_2$, the Se atom is surrounded by two Cu and two Ga atoms, so the initial site symmetry around Se is already C_2 (monoclinic). While Cu-Cu, Cu-Ga, or Ga-Ga dimers are possible, we find that only Ga-Ga dimer bonds form. The reason is that the energies of the $4s$ and $4p$ atomic orbitals, from which the dangling bonds are constructed, decrease along the Cu → Zn → Ga sequence, and, consequently, the Ga-Ga dimer is more stable than the Cu-Ga or Cu-Cu dimers. The structural configurations around the relaxed neutral Se vacancy in ZnSe and CuGaSe$_2$ are given in Table I and illustrated in the lower
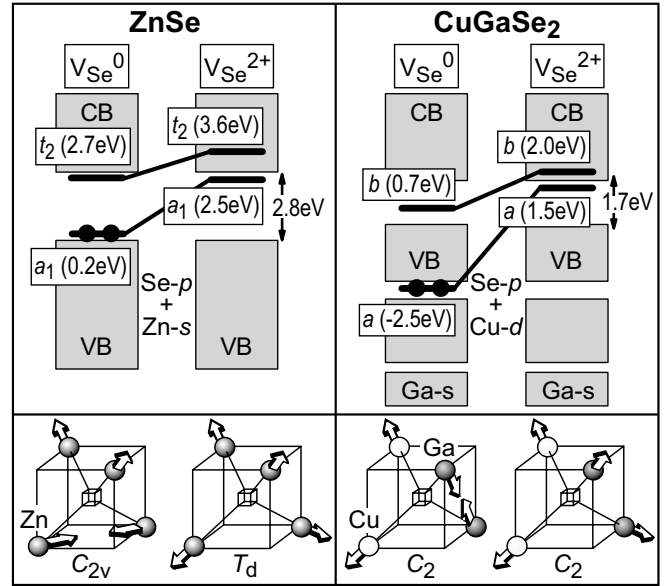
FIG. 1. The single-particle energies of the a_1 (a) vacancy orbitals in ZnSe (CuGaSe$_2$) with respect to the host band structure, for the neutral and the 2+ state using experimental lattice constants. The higher energy t_2 (b) orbitals are also shown for completeness. (The splitting of the t_2 orbital in the C_{2v} symmetry is small and, therefore, omitted). In the lower panel, the relaxation pattern and point-group symmetry corresponding to the different charge states are indicated.

panel of Fig. 1. We see that the metal-metal separation in the host semiconductor (4.01 Å in ZnSe and 3.93 Å in CuGaSe$_2$) is greatly reduced after V_{Se}^0 is formed, leading to the creation of Zn-Zn dimers in ZnSe (bond length: 2.52 Å), and Ga-Ga dimers in CuGaSe$_2$ (2.83 Å). Since the a_1^2 orbital of V_{Se}^0 is nondegenerate, the Jahn-Teller effect can not explain the lowering of symmetry from T_d to C_{2v} in ZnSe. Rather, it is the chemical stability (formation of deep bonding orbitals) of these metal-metal bonds that drives the dimer formation.

Relaxation-induced energy lowering of defect levels— The large, symmetry-lowering atomic relaxations of V_{Se}^0 lead to profound changes in the electronic structure, low-

TABLE I. The closest metal-metal distance (M = Zn, Ga) and the relaxation energy, i.e., the energy gain due to relaxation from ideal lattice positions, for V_{Se}^0 and V_{Se}^{2+} in ZnSe and in CuGaSe$_2$. In CuGaSe$_2$, the Cu atoms move outwards to an almost planar configuration in all charge states of V_{Se}, having a Cu-Cu distance of about 4.9 Å.

			ZnSe			CuGaSe$_2$	
		host	T_d	C_{3v}	C_{2v}	C_2	host
V_{Se}^0	$d_{M\text{-}M}$[Å]	4.01	3.63	3.05	2.52	2.83	3.93
	ΔE_{rel}[Å]		0.14	0.30	0.46	0.92	
V_{Se}^+	$d_{M\text{-}M}$[Å]	4.01	4.58	⋯	⋯	⋯	
	ΔE_{rel}[Å]		0.42	⋯	⋯	⋯	
V_{Se}^{2+}	$d_{M\text{-}M}$[Å]	4.01	5.06	⋯	⋯	5.29	3.93
	ΔE_{rel}[Å]		1.90	⋯	⋯	1.02	

ering the single-particle energy of the $a_1(a)$ orbital in ZnSe (CuGaSe$_2$) from $E_v + 1.1$ eV ($E_v + 0.2$ eV), before relaxation to $E_v + 0.2$ eV ($E_v - 2.5$ eV), after relaxation. Thus, as illustrated in the upper panel of Fig. 1, after relaxation, the doubly occupied a_1^2 level is located in ZnSe just above the VBM, whereas in CuGaSe$_2$ it is deep *inside* the valence band. When V_{Se}^0 is ionized twice, we form the a_1^0 configuration of V_{Se}^{2+} (Fig. 1), showing a breakup of the metal-metal dimers (Table I), and a return to the original T_d lattice symmetry (Fig. 1, bottom). The single-particle energy level of the a_1 state in ZnSe moves *up* from $E_v + 0.2$ eV (V_{Se}^0) to $E_v + 2.5$ eV (V_{Se}^{2+}), whereas in CuGaSe$_2$ it moves *up* from $E_v - 2.5$ eV (V_{Se}^0) to $E_v + 1.5$ eV (V_{Se}^{2+}) [20]. That atomic relaxation is the driving force for this level shift can be judged from the fact that electrostatic effects, i.e., the relief of interelectronic Coulomb repulsion due to the a_1^2 (V_{Se}^0) $\rightarrow a_1^0$ (V_{Se}^{2+}) transition, would have displaced the a_1 level towards *lower* energies. Because of the charge state dependent shift of the defect level from *below* VBM to *above* the VBM, the Se vacancy in chalcopyrites can assume a metastable configuration, in which electrons are transferred from the VBM to the deep defect level, releasing free holes. Thus, the Se vacancy can explain the persistent photoconductivity observed in experiment [12], constituting the unusual case in which a donorlike defect causes p-type persistent photoconductivity.

The singly ionized V_{Se}^+ (a_1^1) center in ZnSe has tetrahedral symmetry (cf. Table I), and the a_1 level is located at $E_v + 1.8$ eV. This charged state is unstable against charge disproportion $2V_{Se}^+ \rightarrow V_{Se}^0 + V_{Se}^{2+}$, in agreement with Refs. [5,6]. Thus, the Se vacancy in ZnSe is a "negative-U defect", with $U = -0.81$ eV being the energy balance of the above reaction. Since, however, the disproportion is associated with considerable energy barriers, it is possible to create V_{Se}^+ in ZnSe temporarily by optical excitation. This is important for the possibility of observing V_{Se}^+ in the EPR experiments discussed below. The situation is qualitatively different in CuGaSe$_2$: The singly occupied a^1 level of V_{Se}^+ lies *below* the VBM. Thus, this level becomes automatically doubly occupied, transforming V_{Se}^+ (a^1) spontaneously into a neutral vacancy V_{Se}^0 (a^2) and releasing a hole to the valence band ($V_{Se}^+ \rightarrow V_{Se}^0 + h$). Thus, in contrast to ZnSe, in CuGaSe$_2$ V_{Se}^+ is not even locally stable.

Deep donor transition energies— Figure 2 shows the defect formation energy ΔH_f as a function of the Fermi level E_F in the Se-poor regime. The intersection points where the formation energies ΔH_f of two charge states q and q' are equal (Fig. 2) mark the thermal transition energies $\epsilon(q/q')$. We see from Fig. 2 that (i) the formation energy of the neutral V_{Se}^0 in both materials is above 2 eV, so that the *neutral* vacancy is not abundant even under Se-poor conditions. (ii) The $\epsilon(2+/0)$ donor transition, which releases simultaneously two electrons to the conduction band, occurs at $E_v + 1.34$ eV($= E_C -$
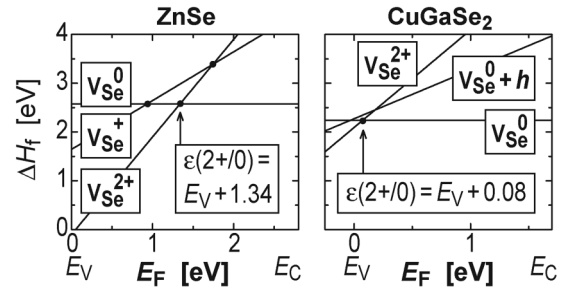

FIG. 2. The formation energy ΔH_f vs Fermi level E_F for the different charge states of the Se vacancy in ZnSe and CuGaSe$_2$. Energies refer to Se-poor conditions; the Se chemical potential with respect to solid Se is $\Delta\mu_{Se} = -1.42$ eV(ZnSe) and $\Delta\mu_{Se} = -0.75$ eV(CuGaSe$_2$). Since, according to the LDA calculation, V_{Se}^+ transforms in CuGaSe$_2$ spontaneously to a neutral vacancy plus a free hole, the energy of $V_{Se}^0 + h$ is shown, too. Numbers include the image charge correction of Ref. [19]. Neglecting this correction gives $\epsilon(2+/0) = E_v + 1.59$ eV and $E_v + 0.32$ eV in CuGaSe$_2$.

1.46 eV) in ZnSe and $E_v + 0.08$ eV($= E_C - 1.62$ eV) in CuGaSe$_2$, i.e., in the lower half of the band gap. Calculations for V_{Se} in CuInSe$_2$ yield also a thermal transition energy very close to VBM, resulting from a similar relaxation pattern as discussed for CuGaSe$_2$. Thus, the Se vacancy is a deep defect in ZnSe, CuGaSe$_2$, and CuInSe$_2$, and can not provide electrons to the CB by thermal ionization. This result is in marked contrast to the common belief, expressed, in particular, for the chalcopyrite semiconductor CuInSe$_2$ [8,10–12]. Regarding the identity of the native donor that produces n-type conductivity in CuInSe$_2$ under appropriate growth conditions [8,12], we rule out the Se vacancy due to the very large ionization energy. Recent work suggests that In$_{Cu}$ is a likely candidate [25].

Predicting vacancy optical excitations— Experimentally, two optical absorption bands related to the anion vacancy were observed in ZnS [14] and ZnSe [15]: First, illumination into the higher energy absorption band, which was associated with unspecified defects [14,15], increased the intensity of the EPR active, spin $1/2$ state V_{anion}^+ of the vacancy. Illumination into the second, lower energy band, identified with the V_{anion}^+ level itself [14,15], caused quenching of the EPR. Figure 3 illustrates schematically the optical transitions that can cause excitation and quenching of the EPR active V_{anion}^+ state. We next show that our calculated *deep* vacancy levels explain both observed bands rather simply without the need to invoke additional unspecified defects. We calculate the optical (vertical) transition energies from total-energy differences, fixing the relaxed atomic positions of the initial state according to the Franck-Condon principle. (i) The $a_1^2 \rightarrow a_1^1 + e$ ($V_{Se}^0 \rightarrow V_{Se}^+ + e$) transition, labeled $\epsilon_o(0/+; e)$ in Fig. 3, in which the first electron is excited from the vacancy level to the conduction band, creating the EPR active 1+ state: Because of
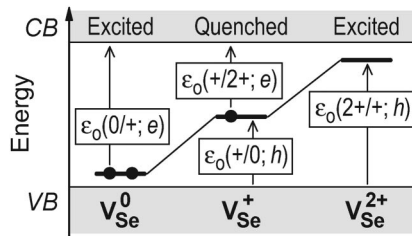
FIG. 3. Optical transitions for V_{Se} in ZnSe. The labels "Excited" and "Quenched" describe whether the EPR active V_{Se}^{+} state is excited or quenched by the respective transitions.

the low energy of the a_1^2 state close to the VBM (cf. Figure 1), the calculated transition energies $\epsilon_o(0/+;e) = 3.49$ eV (ZnS) and 2.66 eV (ZnSe) equal almost the band gap energy. These values agree well with the respective absorption bands with the onset at 3.3 eV (ZnS, Ref. [14]) and 2.4 eV (ZnSe, Ref. [15]). (ii) The $a_1^1 \rightarrow a_1^0 + e$ ($V_{Se}^{+} \rightarrow V_{Se}^{2+} + e$) transition, labeled $\epsilon_o(+/2+;e)$ in Fig. 3, in which the second electron is excited to the CB: The calculated transition energies $\epsilon_o(+/2+;e) = 2.59$ eV and 1.59 eV again compare well with the experimental photon energies of 2.6 eV (ZnS, Ref. [14]) and 1.7 eV (ZnSe, Ref. [15]), which result in quenching of the EPR signal and bleaching of the coloration. The $\epsilon_o(+/0;h)$ and $\epsilon_o(2+/+;h)$ transitions, shown in Fig. 3, correspond to the excitation of an electron from the valence band into the defect state. We calculated also the $\epsilon_o(+/0;h)$ transition, being 2.19 and 1.97 eV in ZnS and ZnSe, respectively. However, the EPR quenching spectra do not show transitions at these energies [14,15]. In the case of the neutral sulfur vacancy in ZnS, the orthorhombic relaxation mode is again found to be the most stable configuration, indicating that the metal-metal-dimer bond formation next to the anion vacancy is a rather general phenomenon in II-VI and chalcopyrite semiconductors. The good agreement between the calculated optical transition energies with the experimental data confirms that the energies of these localized *donor* orbitals have to be referred to the *valence* band states rather than the conduction band states, thus validating the above described way to correct the LDA band gap error.

In summary, nonsymmetric atomic relaxation patterns induced by the formation of stable metal-metal-dimer bonds are identified as the energetically favorable reconstruction of the neutral anion vacancy in all investigated semiconductors; ZnSe, ZnS, CuGaSe$_2$, and CuInSe$_2$. Such atomic relaxations significantly alter the energy of the defect orbitals, rendering the anion vacancy a deep defect. Our results highlight the fact that changes in charge state can be associated with activated structural transformations. The optical transitions arising from the vacancy levels explain the illumination behavior of the color center in ZnSe and ZnS without the need to assume interaction with additional defects.

[1] *Vacancies and Interstitials in Metals and Alloys*, edited by H. Wollenberger and C. Albromeit (Trans Tech, Aedermannsdorf, 1987).

[2] M. Lannoo and J. Bourgoin, *Point Defects in Semiconductors I* (Springer, New York, 1981); A. M. Stoneham, *Theory of Defects in Solids: Electronic Structure of Defects in Insulators and Semiconductors* (Oxford University, New York, 2001).

[3] M. Lannoo and A. M. Stoneham, J. Phys. Chem. Solids **29**, 1987 (1968).

[4] H. L. Hartnagel *et al.*, *Semiconducting Transparent Thin Films* (Institute of Physics, Bristol, 1995).

[5] A. García and J. E. Northrup, Phys. Rev. Lett. **74**, 1131 (1995).

[6] S. Pöykkö, M. J. Puska, and R. M. Nieminen, Phys. Rev. B **57**, 12 174 (1998).

[7] G. D. Mahan, J. Appl. Phys. **54**, 3825 (1983).

[8] S. M. Wasim, Solar cells **16**, 289 (1986).

[9] A. Yamada *et al.*, J. Appl. Phys. **81**, 2794 (1997).

[10] S. H. Wei, S. B. Zhang, and A. Zunger, J. Appl. Phys. **85**, 7214 (1999).

[11] M. A. Contreras *et al.*, Inst. Phys. Conf. Ser. **152**, 333 (1998).

[12] U. Rau and H. W. Schock, Appl. Phys. A **69**, 131 (1999).

[13] G. D. Watkins, in *Electronic Structure and Properties of Semiconductors*, edited by W. Schröter (VCH, Weinheim, 1991), p. 105.

[14] J. Schneider and A. Räuber, Solid State Commun. **5**, 779 (1967); K. Leutwein, A. Räuber, and J. Schneider, Solid State Commun. **5**, 783 (1967).

[15] I. A. Gorn *et al.*, Sov. Phys. Semicond. **24**, 336 (1991); S. Kishida *et al.*, Phys. Status Solidi A **95**, 155 (1986).

[16] J. Ihm, A. Zunger, and M. L. Cohen, J. Phys. C **12**, 4409 (1979).

[17] (a) D. M. Ceperley and B. J. Alder, Phys. Rev. Lett. **45**, 566 (1980); (b) J. P. Perdew and A. Zunger, Phys. Rev. B **23**, 5048 (1981).

[18] G. Kresse and J. Furthmüller, Comput. Mater. Sci. **6**, 15 (1996); G. Kresse and J. Joubert, Phys. Rev. B **59**, 1758 (1999).

[19] G. Makov and M. C. Payne, Phys. Rev. B **51**, 4014 (1995).

[20] If instead of using the experimental lattice constant a_0, we use the smaller a_0 obtained by LDA, we find changes in the formation and single-particle energies in the order of 0.3 eV and the energy gain of the C_{2v} over the T_d configuration of V_{Se}^0 (cp. Table I) is reduced from 0.32 to 0.09 eV. Using the generalized gradient approximation (larger a_0) gives again a larger gain of 0.26 eV.

[21] A. I. Liechtenstein, V. I. Anisimov, and J. Zaanen, Phys. Rev. B **52**, R5467 (1995).

[22] C. J. Vesely, R. L. Hengehold, and D. W. Langer, Phys. Rev. B **5**, 2296 (1972); L. Ley *et al.*, Phys. Rev. B **9**, 600 (1974).

[23] J. E. Jaffe and A. Zunger, Phys. Rev. B **29**, 1882 (1984).

[24] The shallow transition level calculated by Wei, Zhang, and Zunger [10] for V_{Se} in CuInSe$_2$ reflects a different method ($X\alpha$) to correct for the LDA band gap error.

[25] S. Lany, Y. J. Zhao, C. Persson, and A. Zunger (to be published).